Hybrid power quality conditioner for co-phase power supply system in electrified railway

N.Y. Dai   K.W. Lao   M.C. Wong   C.K. Wong

Department of Electrical and Computer Engineering, Faculty of Science and Technology, University of Macau,
Av. Padre Tomás Pereira, Taipa, Macau, People's Republic of China
E-mail: nydai@umac.mo

Abstract: Power quality conditioners based on modern power electronics technology were proposed to solve the power quality problems of the electrified railway power supply system. Large-capacity power converters are used as the main circuits of the compensator, which is one of the main reasons for the high initial cost of the railway power conditioner. A hybrid power quality conditioner (HPQC) for co-phase power supply system in electrified railway is proposed in this study. The HPQC adopts a single-phase back-to-back converter. It connects to the feeding phase of the balance feeding transformer via an $L–C$ branch and to the other phase via a coupling transformer. To inject the same compensating currents to the traction power supply system, the DC bus voltage of the HPQC could be much lower than that of an active power conditioner (APC). As a result, the cost of the power quality conditioner is reduced. Simulation models are built with a HPQC connected to the secondary side of a 110 kV/27.5 kV V/V transformer. Simulation results show the HPQC could compensate reactive current, unbalance current and current harmonics simultaneously. Comparisons with an APC are also given. A small-capacity experimental prototype is built in the laboratory to validate the HPQC and testing results are also provided.

Nomenclature

v_A, v_B, v_C	voltage at primary side of traction transformer
v_α, v_β	voltage at secondary side of traction transformer
i_A, i_B, i_C	currents at the primary side of traction transformer
i_a, i_b, i_c	currents at the secondary side of traction transformer
i_L	current of traction loads
i_{L1p}, i_{L1q}	active and reactive component of fundamental frequency component of load current
i_{Lh}	harmonic component of traction load current
i_{pa}, i_{pb}, i_{pc}	compensating currents inject to the secondary side of traction transformer
$\cos \varphi_1$	displacement power factor of traction load
K	the ratio of turns of traction transformer
i_{pa_set}	the fundamental frequency compensating current of phase A under a set load condition
$V_{inv\alpha}$, $V_{inv\beta}$	output voltage of α-phase and β-phase converter
$V_{inv\alpha 1}$	fundamental frequency component of output voltage of α-phase converter
$V_{inv\alpha h}$	harmonic component of output voltage of α-phase converter
X_{LC}	coupling impedance between α-phase converter and supply system
V_{LC}	voltage across coupling impedance at α-phase
X_L	coupling impedance between β-phase converter and supply system
V_L	voltage across coupling impedance at β-phase

1 Introduction

The 25 kV single-phase AC supply has been widely adopted in the long-distance electrified railway in many countries. The electrical locomotives generate reactive power and harmonic currents in traction power supply systems. The single-phase traction loads also inject large unbalance currents to the three-phase power grid and cause voltage unbalance subsequently. As the amount of rail traffic increases, the issue of power quality distortion becomes more critical [1–3].

In 1990s, balance feeding transformers are used in a few traction power supply substations (SSs) in China. The system configuration of traditional traction power system is shown in Fig. 1. There are several balance transformers, such as Scott, YNvd, V/V and impedance balancing transformers [4–6]. Among them, the V/V transformer has the simplest structure. These transformers could convert the three-phase supply into two single-phase voltage sources, which supply two neighbouring sections, respectively. Unbalance currents could be reduced under this supply mode. However, perfect compensation of the unbalance
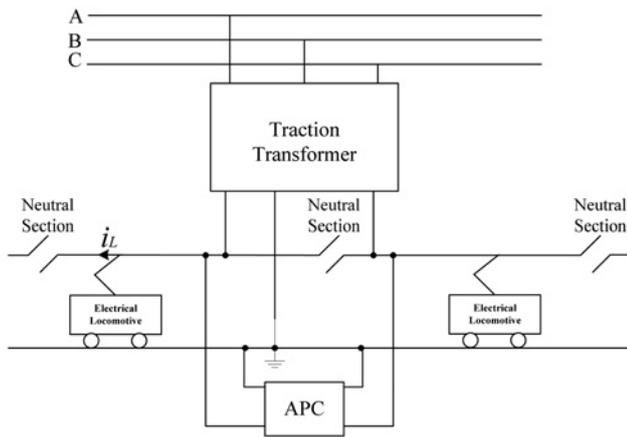
Fig. 1 *Traditional traction power supply*

Fig. 2 *Co-phase traction power supply*

currents could only be achieved when the currents of the two phases at the secondary side are balanced. The chances of having equal loads are very small. In addition, the harmonics and reactive currents from the traction loads could not be compensated. Compared to passive compensation techniques, active compensators could compensate more than one power quality distortion simultaneously and have better dynamic performance. Field testing results of the railway static power conditioner in Shinkansen in Japan were reported around 2004 [7]. Studies about using active power conditioners (APCs) to operate together with the balance transformer could be found in [8–11]. Recently, the multi-level converter for railway power quality conditioner has been studied [12, 13].

As shown in Fig. 1, the traction power system is separated into electrically isolated sections with length of 20–30 km by neutral section (NS). Each section is separately fed from a single-phase voltage supply. The length of the NS varies from several hundred metres to more than 1 km. The fact that electric locomotive needs to slide across the NS without power supply, affects its speed and may make the passengers feel uncomfortable. In addition, expensive automatic switches and their controllers are required for switching the power supply of the locomotive at each NS [14, 15].

As more heavy-load high-speed trains are put into use in China, more distortion currents are injected to the supply system. At the same time, it is preferred that these new trains have a continuous supply without interruption. Therefore the co-phase traction power supply systems with balance transformer and active power compensator were proposed so as to feed the single-phase traction loads without the three-phase side voltage unbalance and distortion [12, 16–19]. The number of NSs could be cut down by half in the co-phase power supply system. The remained NS can be replaced by section insulator, for which the requirement of insulation is reduced since the terminal voltage difference between the two neighbouring sections is much smaller. The configuration of the co-phase power supply system is shown in Fig. 2, in which a V/V transformer is used as the balance feeding transformer. Other balance feeding transformers are also applicable, but the current relationships on the primary side and secondary side are different because of transformer winding connections. The two outputs of the balance feeding transformer supply the same section in the co-phase power supply. As a result, the maximum rating of the locomotive
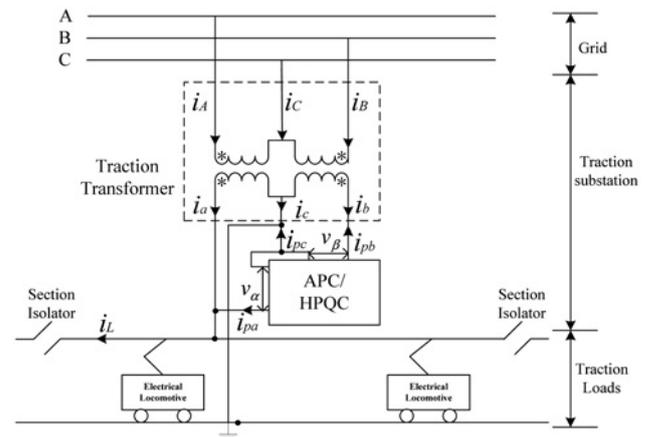
on each section is doubled without increasing the capacity of the traction transformer.

In the co-phase power supply system, one phase at the secondary side of the traction transformer directly supplies the traction loads. The other phase supplies the loads indirectly via a power conditioner. The single-phase back-to-back converter is adopted in the power conditioner, which could balance the active currents between the transformer's two secondary windings. Since one side of the power conditioners is connected in parallel with the traction loads, both the harmonic and the reactive powers at the load side are compensated simultaneously. However, the ratings of the power converter in the power quality conditioner for the co-phase power supply system could be larger than 10 MVA. The initial cost of the power converter is around USD60 per kVA whereas the passive filter only requires USD5 per kVA [12]. Therefore the high initial cost is the main obstacle for promoting the co-phase power supply system.

In this paper, a novel hybrid power quality conditioner (HPQC) is proposed for the co-phase power supply system. The HPQC can achieve active power balancing, reactive power compensation and harmonic filtering as pure APC in the co-phase power supply system. However, the rating of the back-to-back converter can be lower. It is estimated that about 30% of the initial cost of the converter can be saved. Since the power converter in railway power compensator ranges from several MVA to more than 10 MVA, a large amount of money could be saved. In Section 2, the system configuration and the operational principle of the co-phase power supply system are provided. The ratings of the power converters in HPQC are analysed in Section 3. The control system is implemented in Section 4. Simulation verification and comparisons with pure APC are provided in Section 5. Experimental results are given in Section 6.

2 Operational principle of the co-phase power supply system

The system configuration of the co-phase power supply system is given in Fig. 2, in which a V/V transformer is selected owing to its low cost and simple connection. If the proposed co-phase power supply with power quality conditioner could work, the three-phase currents at the grid side would be balanced and in phase with the voltages. Based on this assumption, the compensating currents of the power conditioner are deduced.

It is assumed that the three-phase voltages at the grid side are expressed as

$$\begin{bmatrix} v_A \\ v_B \\ v_C \end{bmatrix} = \begin{bmatrix} \sqrt{2}V_A \sin \omega t \\ \sqrt{2}V_A \sin(\omega t - 120°) \\ \sqrt{2}V_A \sin(\omega t + 120°) \end{bmatrix} \quad (1)$$

The voltage at the secondary side of the V/V transformer is expressed in (2), in which v_α directly supplies the electric traction loads

$$\begin{bmatrix} v_\alpha \\ v_\beta \end{bmatrix} = \begin{bmatrix} v_{ac} \\ v_{bc} \end{bmatrix} = \begin{bmatrix} \sqrt{2}V_{ac} \sin(\omega t - 30°) \\ \sqrt{2}V_{bc} \sin(\omega t - 90°) \end{bmatrix} \quad (2)$$

Without the power conditioner, the load current at the secondary side of the traction transformer is

$$\begin{bmatrix} i_a \\ i_b \\ i_c \end{bmatrix} = \begin{bmatrix} i_L \\ 0 \\ -i_L \end{bmatrix} \quad (3)$$

Load current is divided into the fundamental frequency component, i_{L1}, and the harmonic component, i_{Lh}, as in

$$i_L = i_{L1p} + i_{L1q} + i_{Lh} \quad (4)$$

where i_{L1p} and i_{L1q} are, respectively, the active component and the reactive component of the load current, and could be expressed as

$$i_{L1p} = \sqrt{2}I_{L1p} \sin(\omega t - 30°) \quad (5)$$

$$i_{L1q} = -\sqrt{2}I_{L1q} \cos(\omega t - 30°) \quad (6)$$

where $I_{L1p} = I_{L1} \cos \varphi_1$ and $I_{L1q} = I_{L1} \sin \varphi_1$. φ_1 denotes the phase angle between the supply voltage and the fundamental frequency current of the traction load. The active power consumed by the traction load is

$$P_L = V_\alpha I_{L1} \cos \varphi_1 = V_\alpha I_{L1p} \quad (7)$$

If the power quality conditioner works, compensating currents are injected

$$\begin{bmatrix} i_a \\ i_b \\ i_c \end{bmatrix} = \begin{bmatrix} i_L - i_{pa} \\ -i_{pb} \\ -i_L - i_{pc} \end{bmatrix} \quad (8)$$

The currents at grid side are balanced and with unity power factor, as given in

$$\begin{bmatrix} i_A \\ i_B \\ i_C \end{bmatrix} = \begin{bmatrix} \sqrt{2}I_A \sin \omega t \\ \sqrt{2}I_A \sin(\omega t - 120°) \\ \sqrt{2}I_A \sin(\omega t + 120°) \end{bmatrix} \quad (9)$$

The three-phase grid only provides active power to the traction loads and the power is expressed as

$$P_S = 3V_A I_A \quad (10)$$

Since the load active power is provided by three-phase grid, the power in (7) and (10) should be equivalent, that is, $P_S = P_L$. In addition, $V_\alpha = V_A \times \sqrt{3}/K$, where K is the ratio of turns of the traction transformer. The root mean square (rms) value of the source current could be deduced

$$I_A = \frac{1}{\sqrt{3}K} I_{L1p} \quad (11)$$

It is assumed that the current harmonics are compensated at the secondary side of the traction transformer, that is to say, there is no harmonics passing through the transformer. The compensating currents of the power conditioner are given in

$$\begin{bmatrix} i_{pa} \\ i_{pb} \\ i_{pc} \end{bmatrix} = \begin{bmatrix} i_L \\ 0 \\ -i_L \end{bmatrix} - K \begin{bmatrix} i_A \\ i_B \\ i_C \end{bmatrix} \quad (12)$$

By substituting (4)–(6), (9) and (11) into (12), equation (13) is obtained. The compensating currents are constructed by the fundamental frequency component being in phase with voltage, and being perpendicular to voltage and harmonics (see (13))

If the power conditioner could inject the compensating currents in (13) at the secondary side of the V/V transformer, the reactive current, the unbalance current and the harmonic currents are compensated simultaneously and the grid side currents become balanced with unity power factor.

3 Capacity optimisation of the HPQC

The topology of the proposed HPQC is shown in Fig. 3, in which the DC capacitor illustrates the energy exchanged via the DC part. The topology of the DC bus varies according to the converter structure. The α-phase converter is connected in parallel with the traction loads and the β-phase converter is connected to the other phase of the V/V transformer.

In previous study [7, 17], coupling transformer is used to reduce the voltage rating of the power converter. However, the current rating increases and the total rating of the converter remains the same. When the multi-level converter is adopted, the voltage rating of the converter is increased so that the α-phase converter could connect to the supply line without the coupling transformer [12]. As a result, the DC bus voltage needs to be larger than the peak value of the supply voltage in order to inject the required compensating currents to the power supply system. In this paper, the HPQC is proposed, which could inject the same compensating current with reduced DC voltage. Hence, the total rating of the power converter is reduced.

$$\begin{bmatrix} i_{pa} \\ i_{pb} \\ i_{pc} \end{bmatrix} = \begin{bmatrix} \frac{1}{2}\sqrt{2}I_{L1p} \sin(\omega t - 30°) - \left(\frac{1}{2\sqrt{3}}I_{L1p} + I_{L1q}\right)\sqrt{2} \cos(\omega t - 30°) + i_{Lh} \\ -\frac{1}{2}\sqrt{2}I_{L1p} \sin(\omega t - 90°) + \frac{1}{2\sqrt{3}}\sqrt{2}I_{L1p} \cos(\omega t - 90°) \\ -i_{pa} - i_{pb} \end{bmatrix} \quad (13)$$
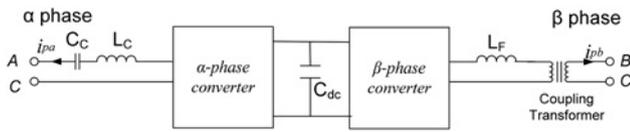
Fig. 3 *Topology of the proposed HPQC*

3.1 Voltage ratings of the α-phase converter

First, the ratings of the α-phase converter are analysed. The α-phase converter is connected to the load side via an $L{-}C$ branch. According to (13), the α-phase converter needs to inject fundamental frequency current both in phase with the supply voltage and perpendicular to the supply voltage in order to compensate the reactive power and unbalance currents at the grid sides. Harmonic compensation is also achieved by the α-phase converter. Based on the superposition algorithm, the equivalent model of the α-phase is decomposed into fundamental frequency model and harmonics model, as shown in Fig. 4. The required voltage rating is first analysed in the fundamental frequency model, then followed by the harmonics compensation.

3.1.1 Fundamental frequency model: The impedance of the $L{-}C$ branch is expressed as (14). Similar to the hybrid power filter [20, 21], the $L{-}C$ branch is resonant at a certain harmonic frequency and its fundamental frequency impedance is capacitive

$$X_{LC} = \frac{1}{\omega C_C} - \omega L_C \qquad (14)$$

In order to inject compensating current to the α-phase, the output voltage of the α-phase converter is expressed as

$$V_{\text{inv}\alpha 1} = V_{\alpha} + V_{LC} = V_{\alpha} - jX_{LC}i_{\text{pa1}} \qquad (15)$$

where i_{pa1} is the fundamental frequency compensating current and V_{LC} is the voltage across the $L{-}C$ branch. According to (14), X_{LC} is a positive value. As shown in Fig. 5, V_{LC} is i_{pa1} rotating $90°$ clockwise. The corresponding vector diagram is shown in Fig. 5.

According to (15), the output voltage of the α-phase converter is determined by the coupling impedance X_{LC} and the compensating current i_{pa1}. First, it is assumed that the
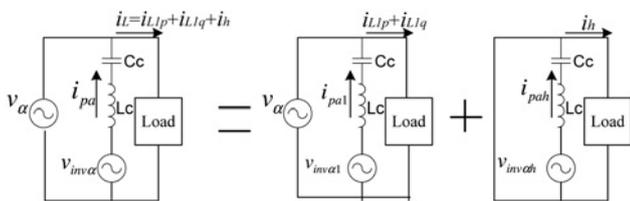

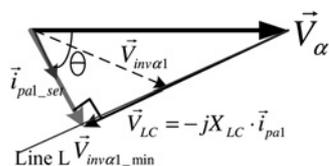**Fig. 4** *Equivalent model of α-phase compensation*

Fig. 5 *Vector diagram for α-phase converter*

HPQC is used to compensate a fixed load and the corresponding compensating current is denoted as $i_{\text{pa1\_set}}$. Given a fixed $i_{\text{pa1\_set}}$, the coupling impedance X_{LC} only changes the amplitude of the output voltage of the α-phase converter, $V_{\text{inv}\alpha 1}$, and it varies along the line L. As shown in Fig. 5, the voltage reaches the minimum value when the vector $V_{\text{inv}\alpha 1}$ is perpendicular to the vector V_{LC} or in phase with vector $i_{\text{pa1\_set}}$. In this case, the coupling impedance equals to

$$X_{LC} = V_{\alpha} \sin\theta / I_{\text{pa1\_set}} \qquad (16)$$

The angle θ is indicated in Fig. 5 and is determined by the compensating current $i_{\text{pa1\_set}}$. According to (13), θ could be calculated by (17), in which $\varphi_1 = \tan^{-1}(I_{L1q}/I_{L1p})$ and it is the angle between the supply voltage V_{α} and fundamental frequency load current i_{L1}

$$
\begin{aligned}
\theta &= \tan^{-1}\left(\left(\frac{1}{2\sqrt{3}}I_{L1p} + I_{L1q}\right) \Big/ \frac{1}{2}I_{L1p}\right) \\
&= \tan^{-1}\left(1/\sqrt{3} + 2\tan\varphi_1\right)
\end{aligned}
\qquad (17)
$$

As a result, the minimum output voltage of the α-phase converter is expressed as

$$V_{\text{inv}\alpha 1\_\min} = \sqrt{V_{\alpha}^2 - (I_{\text{pa1\_set}}X_{LC})^2} = V_{\alpha}\cos\theta \qquad (18)$$

The variation of $\cos\theta$ according to the displacement power factor of the traction loads is shown in Fig. 6. Since the power factors are generally $0.80{-}0.85$ of the electric locomotives widely used in China [22], Fig. 6 shows that the output voltage of the α-phase converter is much smaller than the system voltage when the HPQC is used since $\cos\theta$ is smaller than one. As a result, a smaller DC bus voltage is required in the proposed HPQC.

The rating of the α-phase converter of the conventional APC is analysed in the Appendix. Results indicate that the α-phase converter output voltage of the APC should always be larger than the supply voltage. The corresponding DC bus voltage should be larger than the peak value of the supply voltage. Hence, the power converter of the proposed HPQC has a smaller rating, which could reduce the initial cost of the compensators.

3.1.2 Harmonic model for harmonics compensation: The α-phase converter also works in compensating harmonic currents of the traction loads. It is
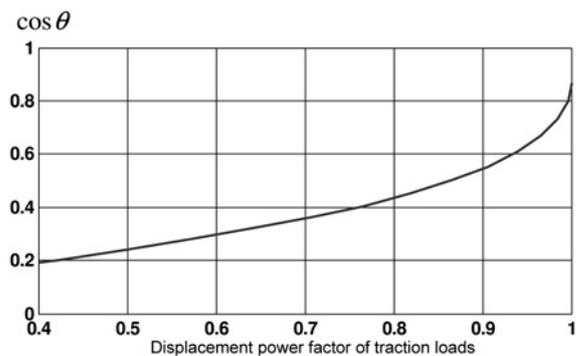

Fig. 6 *Variation of cos θ according to the displacement power factor*

assumed that the harmonic voltage drop across the coupling impedance is mainly generated by the highly current demand and caused by heavy loading. The effect of voltage distortion caused by power supplier is not considered. According to Fig. 4, the output voltage of the α-phase converter is expressed as

$$V_{\text{inv}\alpha h} = V_{ch} = \sqrt{\sum_{h=2}^{\infty} X_{ch}^2 I_h^2} \qquad (19)$$

In the previous part, X_{LC} denotes the fundamental frequency impedance of the coupling circuit. Actually, X_{LC} is the summation of the impedance of the coupling capacitor and the inductor. The $L-C$ branch at the α-phase is designed to be resonant at nth harmonic to eliminate load harmonics. The impedance of the LC coupling circuit at the harmonic frequency is expressed as

$$X_{LCh} = \left(\frac{1}{h} - \frac{h}{n^2}\right)\frac{1}{\omega C} = \frac{n^2/h - h}{n^2 - 1}X_{LC} = r_h X_{LC} \qquad (20)$$

where h denotes the harmonic order. Fig. 7 shows how r_h varies according to h. When r_h is positive, the impedance of the $L-C$ branch is still capacitive, just like the fundamental frequency impedance. When r_h is negative, the impedance of the $L-C$ branch becomes inductive.

The impedance equals zero at the resonant frequency. The zero-crossing point for each curve indicates the coupling impedance changes from capacitive to inductive. The harmonic characteristics of the traction loads are given in [23]. The $L-C$ branch at the α-phase is preferred to be resonant at the fifth harmonics, although the most significant harmonic in the load currents is the third order. As shown in Fig. 7, the impedance increases more quickly with the frequency for the third harmonic resonant $L-C$ branch. As a result, selecting the fifth harmonic resonant $L-C$ branch could reduce the inverter output voltage for compensating high-order harmonics.

As provided in the Appendix, the coupling impedance of the inductor-coupled converter increases linearly with the frequency. Compared to the conventional active power quality conditioner, the $L-C$ resonant branch of the HPQC provides zero impedance for the harmonics at resonant frequency. Its impedance for high-order harmonics also increases relatively slowly. Hence, the HPQC could also reduce the voltage rating of the α-phase converter when harmonic compensation is considered.
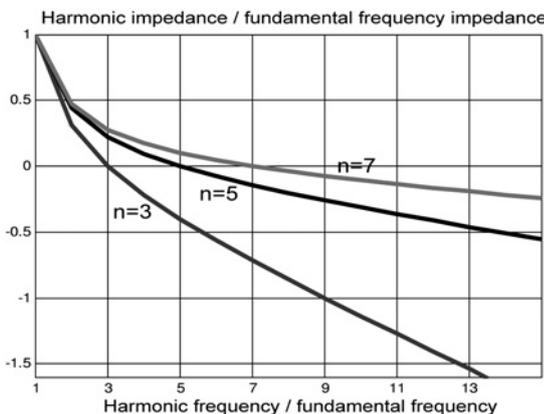

Fig. 7 *r_{xc} varies as frequency increases*

Finally, in order to compensate the reactive current, the unbalance and the harmonics, the rms value of the required output voltage of the inverter could be estimated by

$$V_{\text{inv}\alpha} = \sqrt{V_{\text{inv}\alpha 1}^2 + V_{\text{inv}\alpha h}^2} \qquad (21)$$

However, the peak value of the inverter output voltage is larger than $\sqrt{2}V_{\text{inv}\alpha}$, because the harmonic components are included. Practically, the inverter DC voltage should be larger than $\sqrt{2}V_{\text{inv}\,\alpha}$ to meet the requirement of the power quality conditioning in the co-phase power supply system.

3.2 Voltage ratings for the β-phase converter

According to (13), the compensating current for the β-phase is expressed as

$$i_{pb} = -\frac{1}{2}\sqrt{2}I_{L1p}\sin(\omega t - 90°) + \frac{1}{2\sqrt{3}}\sqrt{2}I_{L1p}\cos(\omega t - 90°) \qquad (22)$$

where $I_{L1p} = I_{L1}\cos\varphi_1$. Unlike the α-phase converter, there is no harmonic compensation requirement for the β-phase. Hence, only the fundamental frequency model is analysed, and the output voltage of the β-phase converter is

$$\boldsymbol{V}_{\text{inv}\beta} = \boldsymbol{V}_\beta + \boldsymbol{V}_L = \boldsymbol{V}_{bc} + jX_L\boldsymbol{i}_{pb} \qquad (23)$$

where $\boldsymbol{V}_L$ is the voltage drop across the coupling inductor and $X_L = \omega L_F$. The vector diagram is shown in Fig. 8. The phase angle of the compensating current vector $\boldsymbol{i}_{pb}$ is given in

$$\delta = \tan^{-1}\left(\frac{1}{2}I_{L1p}\Big/\frac{1}{2\sqrt{3}}I_{L1p}\right) = 60° \qquad (24)$$

The direction of voltage vector across the coupling inductor could be obtained by rotating $\boldsymbol{i}_{pb}$ 90° counter-clockwise. The amplitude of the output voltage of the β-phase converter achieves the minimum value when $\boldsymbol{v}_{\text{inv}\beta}$ is perpendicular to $\boldsymbol{V}_L$, as shown in Fig. 8. Since the phase angle of the β-phase compensating current is a fixed value, the minimum amplitude of $\boldsymbol{v}_{\text{inv}\beta}$ equals to $\sqrt{3}V_\beta/2$. For a small coupling inductor, the voltage rating of the β-phase converter locates in the range of $\sqrt{3}V_\beta/2$ to V_β. The α-phase and the β-phase converter share a common DC bus. However, their converter voltage ratings may not match according to the previous analyses. The ratio of turns of the β-phase coupling transformer could adjust the voltage rating of the β-phase converter and therefore solves this problem. The structure of the conventional APC at the β-phase is the same as that of the HPQC and the converter capacity analyses are almost the same.
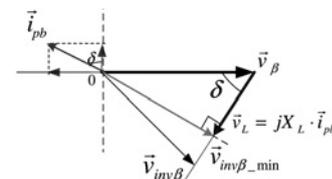

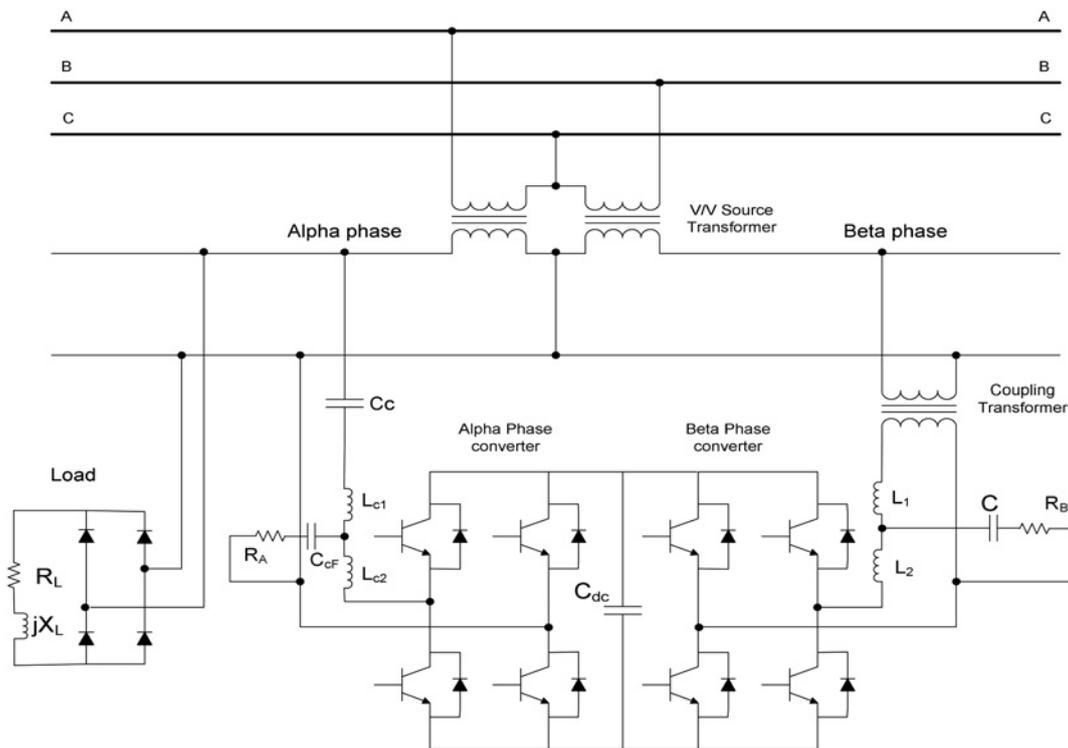**Fig. 8** *Vector diagram for β-phase converter*

Fig. 9 *System configuration of the co-phase power supply system with HPQC*

4 Control system of the HPQC

The system configuration of a co-phase power supply system with HPQC is shown in Fig. 9. A single-phase full-bridge back-to-back converter is adopted to illustrate the operational principle of the proposed system in this section. In order to suppress the current ripples, an LCL filter is used. Practically, a multi-level converter needs to be applied if the α-phase converter is connected to the supply without the coupling transformer. In that case, the LCL filter could be replaced by an inductor.

In order to calculate the reference currents in (13), the instantaneous power method is used. The instantaneous active and reactive powers are calculated by (25), in which v_{ad} and i_{ad} are 90° delay of the system voltage and load current, respectively. The active power is further split into a DC part and an oscillating part, as given in

$$\begin{bmatrix} p \\ q \end{bmatrix} = \begin{bmatrix} v_\alpha i_L + v_{\alpha d} i_{Ld} \\ v_{\alpha d} i_L - v_\alpha i_{Ld} \end{bmatrix} \qquad (25)$$

$$p = p_{dc} + p_{ac} \qquad (26)$$

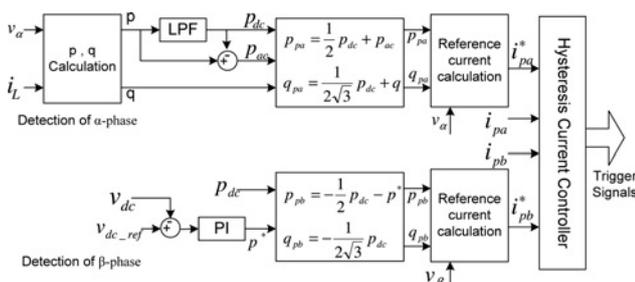The required α-phase and β-phase compensation power can

Fig. 10 *Control system of the HPQC*

be expressed, as in (27). The compensating current of phases A and B is transferred to corresponding power by multiplying the α-phase current by α-phase voltage, and the β-phase current by β-phase voltage

$$\begin{bmatrix} p_{pa} \\ q_{pa} \\ p_{pb} \\ q_{pb} \end{bmatrix} = \begin{bmatrix} \dfrac{1}{2} p_{dc} + p_{ac} \\ \dfrac{1}{2\sqrt{3}} p_{dc} + q \\ -\dfrac{1}{2} p_{dc} \\ -\dfrac{1}{2\sqrt{3}} p_{dc} \end{bmatrix} \qquad (27)$$

Consequently, the reference currents at each phase is calculated by (28) and (29) according to the required output power. Similarly, $v_{\beta d}$ is 90° delay of the system voltage v_β

$$i_{pa}^* = \frac{1}{v_\alpha^2 + v_{\alpha d}^2} \begin{bmatrix} v_\alpha & v_{\alpha d} \end{bmatrix} \begin{bmatrix} p_{pa} \\ q_{pa} \end{bmatrix} \qquad (28)$$

$$i_{pb}^* = \frac{1}{v_\beta^2 + v_{\beta d}^2} \begin{bmatrix} v_\beta & v_{\beta d} \end{bmatrix} \begin{bmatrix} p_{pb} \\ q_{pb} \end{bmatrix} \qquad (29)$$

The obtained reference current signal is sent to the hysteresis current controller. The pulse width modulation signals are generated for the α-phase and β-phase converters, respectively. Fig. 10 illustrates the control diagram of the proposed HPQC. The HPQC balances the grid-side currents by transferring active power between α-phase and β-phase. The β-phase converter absorbs active power from the grid side. If the active power taken by the α-phase is smaller than that provided by the β-phase converter, the DC-link voltage increases and vice versa. Hence, the β-phase

converter also works for DC-bus voltage control. The harmonic compensation is done by the α-phase converter.

As mentioned in the previous part, the DC bus voltage is set according to the rating of the α-phase converter. It is a value smaller than the peak value of the supply voltage since the α-phase converter is connected to the system via a capacitor and an inductor. However, only a coupling inductor is used at the β-phase. Without coupling transformer, the supply voltage is too high to achieve the power transfer at this phase. A step-down coupling transformer is used to reduce the supply voltage at the β-phase. During compensation, active power is transferred from the beta to the alpha phase. For the initial boost-up of the DC link voltage, additional active power is absorbed from the β-phase converter via control. As shown in Fig. 10, the β-phase converter works for DC bus voltage control. This control can also help in maintaining the DC-link voltage during compensation.

5 Simulation verification

Simulations are done by using PSCAD/EMTDC. The system configuration of the co-phase power supply system is shown earlier in Fig. 2. Two 10 MVA 110 kV/27.5 kV transformers
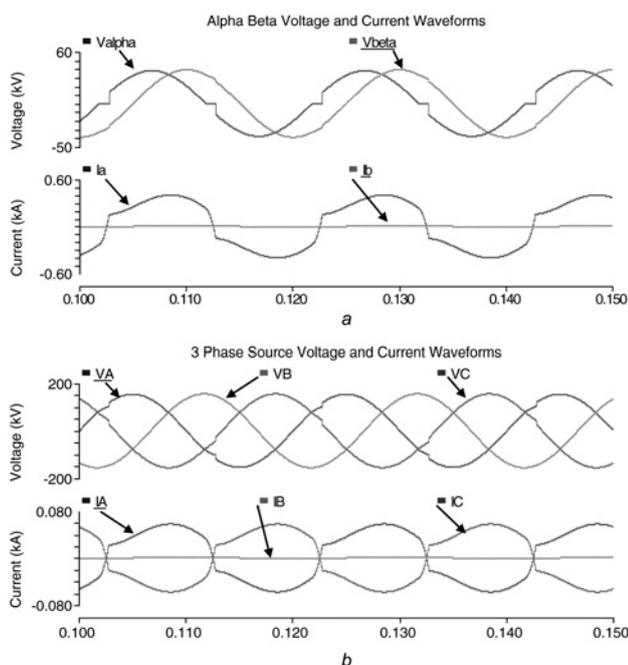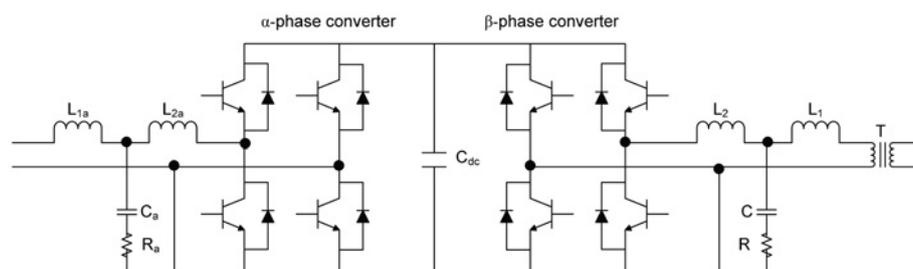
Table 1 Circuit parameters of proposed HPQC in simulation

No.	Items	Description
1	α-phase coupling inductor L_{C1}, L_{C2}	5.945 mH
2	α-phase C_{CF}	5 μF
3	α-phase R_A	30 Ω
4	α-phase coupling capacitor C_α	34.09 μF
5	capacitor C_{dc}	10 000 μF
6	β-phase coupling transformer T	13.75 kV/27.5 kV, 20 MVA (HPQC) 27.5 kV/27.5 kV, 20 MVA (APC)
7	β-phase L_1, L_2	2 mH
8	β-phase C	10 μF
9	β-phase R_B	15 Ω
10	load inductor	193 mH
11	load resistor	80.66 Ω

are used to construct a V/V transformer for the co-phase power supply system. The voltages and currents at the secondary side of the V/V transformer are shown in Fig. 11a without the power quality conditioner. The load is modelled by a single-phase rectifier, as shown in Fig. 9, and its parameters are listed in Table 1. A simplified single-bridge converter could cause higher harmonic distortion problem than either the double-bridge or the multi-bridge. Based on the worst-case consideration, the simplified single-bridge converter is chosen as the traction load model. The current at phase B equals to zero since the load is only connected to the α-phase. The three-phase voltages and currents at the grid side are shown in Fig. 11b.

The conventional co-phase power supply system with APC is first implemented in the simulation. The topology of the APC in simulation is shown in Fig. 12 and the circuit parameters are given in Table 1. The LCL filter is designed according to the method employed in [24, 25]. The DC-link voltage of the power converters in APC should be larger than the peak value of the supply voltage and is 40 kV in simulation. The simulation results are shown in Fig. 13. The APC is connected to the supply system at 0.02 s. The DC-link voltage variation is also provided in Fig. 13. It could be observed that the three-phase source current becomes balanced after compensation, and the harmonics and reactive currents are compensated simultaneously.

The proposed HPQC is also applied to the co-phase power supply system and the system configuration is given in Fig. 9. The coupling capacitor and the inductor at α-phase are tuned to oscillate at the fifth harmonic and are calculated by (14) and (16). The circuit parameters are listed in Table 1. In order to reduce the ripple and high-frequency components in the output of the converter, an LCL filter is adopted at both

Fig. 11 *Co-phase power supply system without power quality conditioner*

a Voltages and currents at the secondary side of the V/V transformer
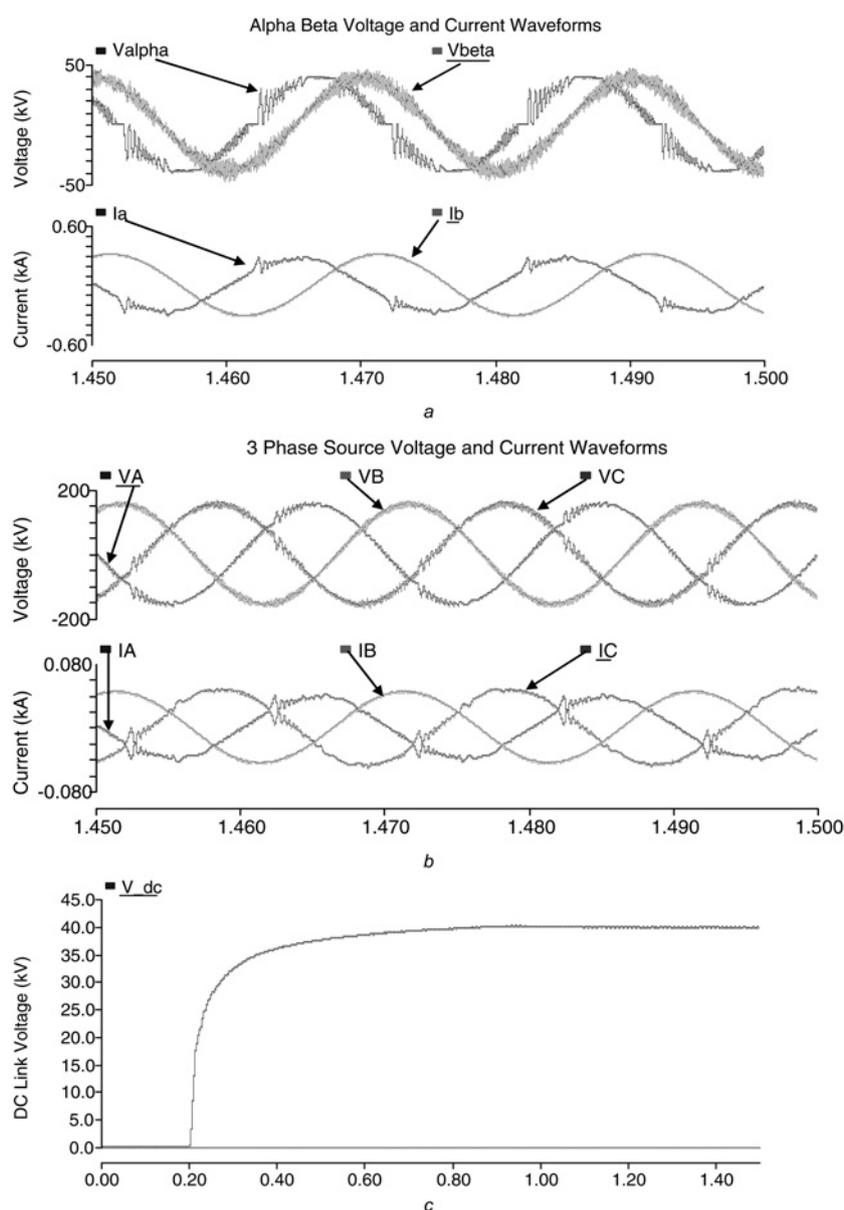*b* Three-phase voltages and currents at the grid side

Fig. 12 *System configuration of the APC*

Fig. 13 *Co-phase power supply system with APC*

a Voltages and currents at the secondary side of the V/V transformer
b Three-phase voltages and currents at the grid side
c APC's DC bus voltage variation

sides of the HPQC in simulation. The DC-link voltage is 28 kV for the HPQC. Simulation results of the co-phase power supply system using HPQC are shown in Fig. 14. The DC-link voltage variation is also provided in Fig. 14.

When Figs. 13 and 14 are compared, results indicate that both structures can be used as the power quality conditioner in the co-phase traction power system. However, the DC-link voltage of the proposed HPQC is only 70% of conventional APC. To further investigate compensation performances, system performances before and after compensations are summarised in Table 2. Total demand distortion (TDD) is used in IEEE standard to evaluate the current distortion [26]. The demand current is set as the full load current of the V/V transformer. The distortion limit for 110 kV line is 2.5%. Results in Table 2 indicate that the compensator fits the requirement of the IEEE standard. In addition, the simulation results of the HPQC when the load varies are given in Fig. 15.

6 Experimental verification

A small-capacity co-phase power supply system with a HPQC was built for verification. The system configuration is the same as Fig. 9, but the LCL filter is replaced by an L filter since the filtering requirement of small-capacity system is lower. The V/V transformer is composed of two 1:1 isolation transformers, with capacity of 5 kVA individually. The peak value of the sinusoidal three-phase supply voltage is 70.7 V. The coupling impedance and coupling transformer parameters are slightly different from the designed value because of practical limitation. The DC-link voltage of the HPQC is 60 V in experiment. The circuit parameters in experiment are listed in Table 3.

Fig. 16 shows the source voltage and source current at grid side, respectively, before and after compensation. The detailed compensation performance is summarised in Table 4. Results indicate that the proposed co-phase power
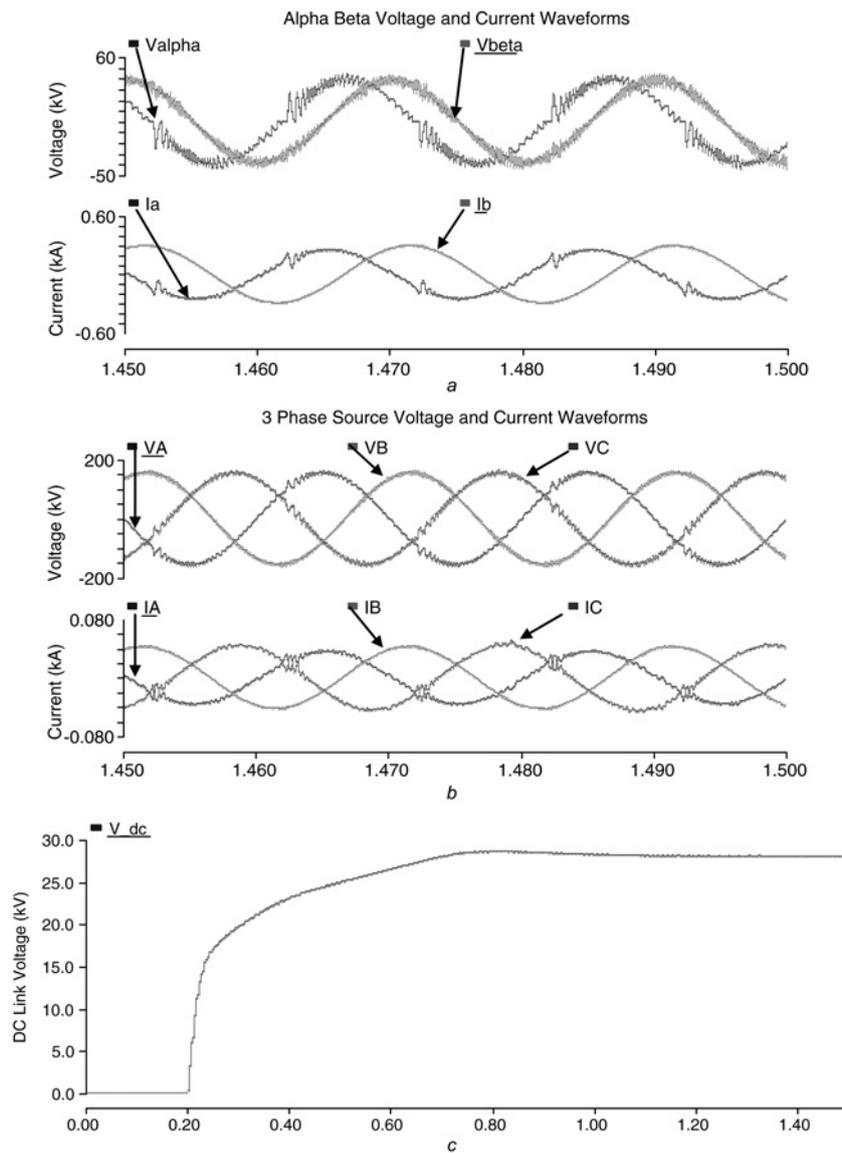
Fig. 14 *Co-phase power supply system with HPQC*

a Voltages and currents at the secondary side of the V/V transformer
b Three-phase voltages and currents at the grid side
c HPQC's DC bus voltage variation

Table 2 Compensation performance comparison using HPQC and APC

Currents	Three-phase source current								
	Before compensation			After compensation using APC (V_{dc} = 40 kV)			After compensation using HPQC (V_{dc} = 28 kV)		
	A	B	C	A	B	C	A	B	C
rms, A	44	0	44	27.5	31.9	33.1	25.8	29.6	31.5
third harmonic, %	14.66	–	14.66	1.85	1.00	1.96	2.42	0.88	1.18
fifth harmonic, %	8.87	–	8.87	3.13	0.27	2.40	0.93	0.18	0.93
seventh harmonic, %	6.06	–	6.06	2.51	0.18	1.86	1.93	0.11	1.65
THD, %	19.2	–	19.2	6.70	1.00	5.49	6.70	0.99	5.52
TDD, %	4.56	–	4.56	1.01	0.18	1.0	0.95	0.16	0.95
current unbalance, %		99			12.34			12.23	

supply system with HPQC could compensate the current unbalance, the reactive current and the current harmonics.

There are difference in simulation and experimental results. The actual component parameters of the circuit, the resolution of the transducers, the digital computation error and the noise may affect the experimental performance. All of the items mentioned above need to be considered in order to improve the practical compensation ability.
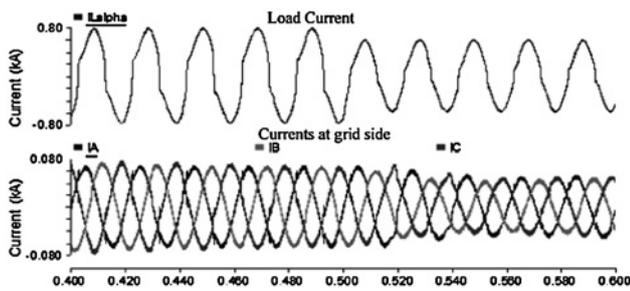
Fig. 15 *Performance of HPQC when load varies*

Table 3 Circuit parameters in experiment

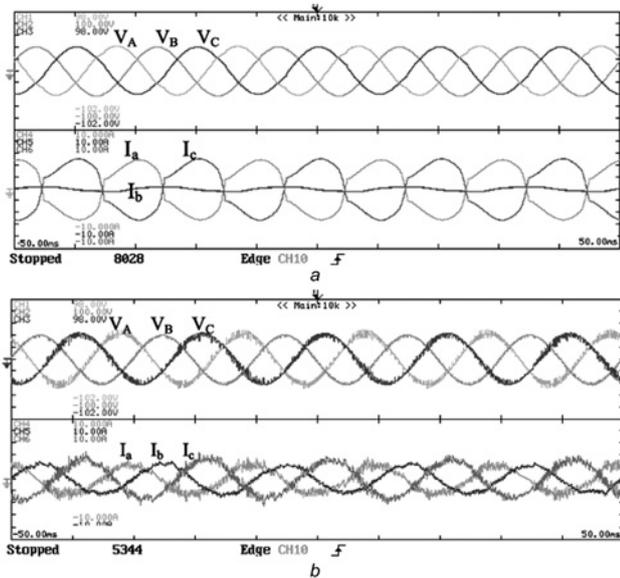| No.	Items	Description
1	α-phase coupling inductor L_a	2.5 mH
2	α-phase coupling capacitor C_a	170 μF
3	DC capacitor	5000 μF
4	coupling transformer T	the ratio of turns:1:2
5	β-phase coupling inductor	12 mH
6	load inductor	30 mH
7	load resistor	10 Ω

Fig. 16 *Co-phase power supply experimental system*
a Voltage and current waveforms before compensation
b Voltage and current waveforms after compensation

7 Conclusions

In this paper, a hybrid power quality compensator is proposed for the co-phase power supply system for electrified railway. The proposed HPQC could operate at a lower DC bus voltage compared to an APC. As a result, the initial cost of the system could be reduced. Simulation results show that the HPQC could compensate reactive current, unbalance current and current harmonics simultaneously. A small-capacity experimental prototype is built in the laboratory to validate the HPQC and testing results are also provided.

8 Acknowledgments

9 References

1 Tan, P., Loh, P.C., Holmes, D.G.: 'Optimal impedance termination of 25-kV electrified railway systems for improved power quality', *IEEE Trans. Power Deliv.*, 2005, **20**, (2), pp. 1703–1710
2 Senini, S.T., Wolfs, P.J.: 'Novel topology for correction of unbalanced load in single phase electric traction systems'. Proc. IEEE Annual Power Electronics Specialists Conf., Cairns, Australia, June 2002, pp. 1208–1212
3 Gao, L., Yonghai, X., Xiangnin, X., Yingying, L., Peisi, J.: 'Analysis of adverse effects on the public power grid brought by traction power-supply system'. Proc. IEEE Electrical Power & Energy Conf., Canada, 2008, pp. 1–7
4 Kuo, H., Chen, T.: 'Rigorous evaluation of the voltage unbalance due to high-speed railway demands', *IEEE Trans. Veh. Technol.*, 1998, **47**, pp. 1385–1389
5 Wang, H., Tian, Y., Gui, Q.: 'Evaluation of negative sequence current injection into the public grid from different traction substation in electrical railways'. Proc. Int. Conf. and Exhibition on Electricity Distribution, Prague, Czech Republic, June 2009, pp. 1–4
6 Dai, C., Sun, Y.: 'Investigation of the imbalance current compensation for transformers used in electric railways'. Proc. Asia-Pacific Power and Energy Engineering Conf. (APPEEC), Chengdu, P.R. China, March 2010, pp. 1–4
7 Uzuka, T., Ikedo, S.: 'Railway static power conditioner field test', *Q. Rep. RTRI*, 2004, **45**, (2), pp. 64–67
8 Zeng, G., Hao, R.: 'Analysis and design of an active power filter for three-phase balanced electrified railway power supply system'. Proc. Int. Conf. on Power Electronics and Drive Systems, Singapore, November 2003, vol. 2, pp. 1510–1513
9 Zhuo, S., Jiang, X., Zhu, D., Ziang, G.: 'A novel active power quality compensator topology for electrified railway', *IEEE Trans. Power Electron.*, 2004, **19**, (4), pp. 1036–1042
10 Horita, Y., Morishima, N., Kai, M., Onishi, M., Masui, T., Noguchi, M.: 'Single-phase STATCOM for feeding system of Tokaido Shinkansen'. Proc. Int. Conf. Power and Energy, Singapore, October 2010, pp. 2165–2170
11 Tanaka, T., Ishibashi, K., Ishikura, N., Hiraki, E.: 'A half-bridge inverter based active power quality compensator for electrified railway'. Proc. Int. Conf. Power Electronics, Sapporo, Japan, June 2010, pp. 1590–1595

Table 4 Compensation performance in experiment

	Three phase source current					
	Before compensation			After compensation		
	A	B	C	A	B	C
rms, A	3.66	0.08	4.01	1.53	1.54	2.32
THD, %	18.9	–	17.5	7.20	5.00	4.60
TDD, %,	2.99	–	3.04	0.48	0.34	0.47
current unbalance, %		99			33.30	

12 Wei, Y.: 'Research on control of comprehensive compensation for traction substations based on the STATCOM technology'. PhD thesis, Tsinghua University, 2009

13 Tan, P.C., Loh, P.C., Holmes, D.G.: 'A robust multilevel hybrid compensation system for 25-kV electrified railway applications', *IEEE Trans. Power Electron.*, 2004, **19**, (4), pp. 1043–1052

14 Han, Z., Liu, S., Gao, S.: 'An automatic system for china high-speed multiple unit train running through neutral section with electric load'. Proc. Asia-Pacific Power and Energy Engineering Conf. (APPEEC), Chengdu, P.R. China, March 2010, pp. 1–3

15 Chen, D., Pan, M., Tian, W., Yang, W.: 'Automatic neutral section passing control device based on image recognition for electric locomotives'. Proc. Int. Conf. Imaging Systems and Techniques (IST), Thessaloniki, Greece, July 2010, pp. 385–388

16 Zhou, F., Li, Q., Qiu, D.: 'Co-phased traction power system based on balanced transformer and hybrid compensation'. Proc. Asia-Pacific Power and Energy Engineering Conf. (APPEEC), WuHan, P.R. China, March 2009, pp. 1–4

17 Shu, Z., Xie, S., Li, Q.: 'Single-phase back-to-back converter for active power balancing, reactive power compensation and harmonic filtering in traction power system', *IEEE Trans. Power Electron.*, 2011, **26**, (2), pp. 334–343

18 Chen, M., Li, Q., Wei, G.: 'Optimized design and performance evaluation of new cophase traction power supply system'. Proc. Asia-Pacific Power and Energy Engineering Conf. (APPEEC), WuHan, P.R. China, March 2009, pp. 1–6

19 Shu, Z., Xie, S., Li, Q.: 'Development and implementation of a prototype for co-phase traction power supply system'. Proc. Asia-Pacific Power and Energy Engineering Conf. (APPEEC), Chengdu, P.R. China, March 2010, pp. 1–4

20 Akagi, H., Hatada, T.: 'Voltage balancing control for a three-level diode-clamped converter in a medium-voltage transformerless hybrid active filter', *IEEE Trans. Power Electron.*, 2009, **24**, (3), pp. 571–579

21 Corasaniti, V.F., Barbieri, M.B., Arnera, P.L., Valla, M.I.: 'Hybrid active filter for reactive and harmonics compensation in distribution network', *IEEE Trans. Ind. Electron.*, 2009, **56**, (3), pp. 670–677

22 Ma, J., Wu, M., Yang, S.: 'The application of SVC for the power quality control of electric railways'. Proc. Int. Conf. Sustainable Power Generation and Supply (SUPERGEN), Nanjing, P.R. China, April 2009, pp. 1–5

23 Gao, L., Xu, Y., Xiao, X., Jiang, P., Zhang, Y.Z.: 'Simulation model and harmonic analysis of SS6B electric locomotive based on PSCAD/EMTDC'. Proc. Conf. Electrical Power Conf. (EPEC), Canada, October 2008, pp. 1–5

24 Vodynakho, O., Mi, C.C.: 'Three-level inverter-based shunt active power filter in three-phase three-wire and four-wire systems', *IEEE Trans. Power Electron.*, 2009, **24**, (5), pp. 1350–1363

25 Han, Y., Khan, M.M., Yao, G., Zhou, L., Chen, C.: 'Design, implementation and field test of a novel hybrid active power filter'. Proc. Int. Conf. Industrial Technology (ICIT), Chengdu, P.R. China, April 2008, pp. 1–6

26 IEEE Std 519-1992: 'IEEE recommended practices and requirements for harmonic control in electrical power systems', 1992

10 Appendix

The capacity for the back-to-back converter in APC is analysed in this part [17]. It is assumed that the same compensating currents are injected into the co-phase power supply system and the minimum required DC bus voltage affects the ratings of the converter.
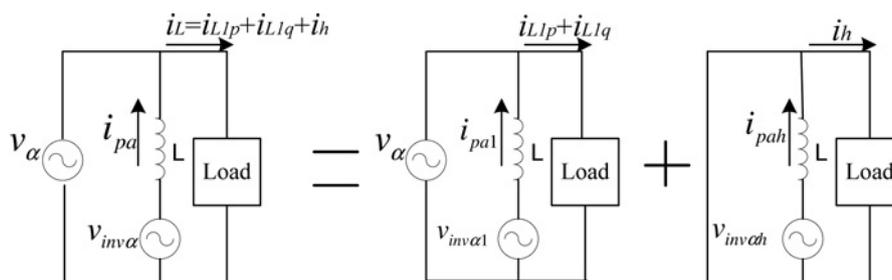
First, the ratings of the α-phase converter are analysed. The α-phase converter is connected to the load side via an inductor. Similar to previous discussions, the equivalent model of the α-phase of the co-phase power supply system is decomposed into fundamental frequency model and harmonics model, as shown in Fig. 17. The fundamental frequency model is first analysed to deduce the voltage rating of the converter. The harmonics compensation will be added as an independent part and can be considered subsequently.

In the fundamental frequency model, the inverter output voltage is expressed as

$$V_{\text{inv}\alpha1} = V_{\alpha} + V_{L} = V_{\alpha} + jX_{L}i_{\text{pa}1} \quad (30)$$

The corresponding vector diagram is shown in Fig. 18. The direction of V_{L} is $i_{\text{pa}1}$ rotates $90°$ counter-clockwise. Since the traction loads are always inductive, in order to provide the required compensation currents, the required voltage rating of the inverter is always larger than V_{α}.

In the harmonic model, the coupling inductance for harmonics is

$$X_{Lh} = hX_{L} \quad (31)$$

The inductor impedance is found to increase linearly with the harmonic order. As a result, the APC needs to provide a larger output voltage for harmonic compensation. The total output voltage of the inverter is calculated according to

$$V_{\text{inv}L} = \sqrt{V_{\text{inv}\alpha1}^2 + \sum_{h=2}^{\infty} X_{Lh}^2 I_{ch}^2} \quad (32)$$

In order to work in the co-phase power supply system, the voltage rating of the APC should always be larger than the supply system voltage. Although the voltage rating could be reduced by using the coupling transformer to integrate the compensator to the supply system, the current rating increases accordingly whereas the rating of the converter always remains the same.
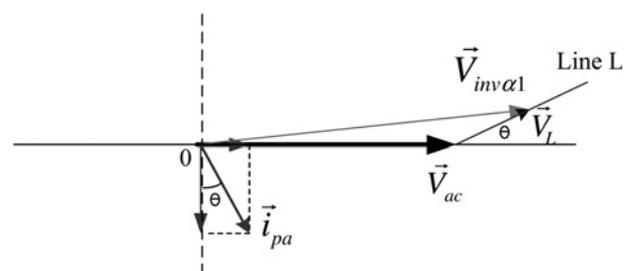

Fig. 18 *Vector diagram of L-coupling UPQC*

Fig. 17 *Equivalent model of α-phase compensation*